# Cost Effective Solitary Stage Single Phase Inverter for Solar PV Integration in to Grid

P.Nammalvar*‡, S.Ramkumar**, R.Umadevi***

*Assistant Professor, Department of Electrical & Electronics Engineering,

Krishnasamy College of Engineering & Technology, Cuddalore, Tamilnadu-607109, India.

**Professor, Department of Electrical & Electronics Engineering,

KPR Institute of Engineering and Technology, Coimbatore, Tamilnadu-641407, India.

***Associate Professor, Department of Electrical & Electronics Engineering,

PSG Institute of Technology and Applied Research, Coimbatore, Tamilnadu-641062, India.

(alvar1976@gmail.com, dean_aa@kpriet.ac.in, umadevi@psgitech.ac.in)

‡Corresponding Author; P.Nammalvar,Assistant Professor/EEE, Krishnasamy college of Engineering & Technology, Cuddalore, Tamilnadu-607109,Tel: +91 9865320077, alvar1976@gmail.com

*Received: 23.03.2018 Accepted:11.02.2018*

**Abstract-** The ambitious plan exhibited in this paper is to develop a single-phase DC/AC grid-integrated, transformerless and cost-effective inverter for solar Photovoltaic (PV) systems. The costly combination of the two converters specifically DC/DC and DC/AC had inspired the development of this new financially cost effective inverter. This novel solitary stage converter has the capability to operate on both buck mode and buck-boost mode to harvest maximum power from two distinctive PV panels with the help of PI and hysteresis controller. The working principle and configuration of the proposed system are verified under equally, as well as incompatible climatological conditions and hence the system can endure a extensive deviation of voltage in both the PV panels. This inverter requires just four switches and is also free from the shoot-through problem. Owing to noticeable features such as dual MPP tracking, omission of transformer, exclusion of diodes, reduced switch count, negligible losses and wide operating voltage, these PV grid-tie inverters continue to work even during periods of partial shading due to clouds or dust. In addition, the viability of the inverter has been validated both by detailed simulation and exhaustive experimental studies on a 230V/50Hz/2000W research centre model.

**Keywords-** Grid integration, Harmonics, Renewable Energy, Solar Photovoltaic, Transformerless Inverter.

## 1. Introduction

With the increasing shortage of coal and petroleum products and growing demand, power generation will stand out as huge challenge for the government and the energy industry in the future. In such a situation, the government may present a proposal that all houses to be installed with PV panels and should produce power for their own purpose, and also, surplus energy can be exported to the grid. Focusing on the high probability of such a situation, this work was begun. Grid-interactive solar PV systems are gradually becoming a more feasible substitute for electricity generation due to technology improvement and drop in component prices in comparison with the escalating cost of fossil fuels. In this paper, an innovative tactic to enhance the energy generated from the PV panels is proposed using novel DC/AC grid tied inverter.

The AC voltage according to the Indian standard is 230V in the distribution grid. Therefore, the DC voltage generated from the PV modules cannot be connected directly to the grid, but must be connected through an inverter. Generally, DC/DC converters are utilized to interface the PV panel, keeping in mind the need to harvest the most energy and DC/AC inverters are utilized for connecting through the grid to inject a sinusoidal current into the grid. In this work, the DC/DC converter is eliminated. Tolerance for an extremely wide range of input voltage variations of the proposed grid-tie inverter is ready to influence the solar power system when run even on cloudy days or during early mornings and late afternoons. Minding the above-mentioned needs, the literature survey was begun on various types of grid-tied inverters suitable for PV applications.

The rapid fashion and increased significance of sustainable power source using solar PV are essential in

rural/urban areas and in industries to meet the mandatory power demand in the recent years. The International Energy Agency (IEA) is the global energy authority with data, analysis and solutions on all fuels. According to a report from the IEA, it is estimated that solar PV Electricity generation is expected to grow by 150% from 2015-2020, and by mid-century, the sun could be the largest wellspring of energy by 2050. The electric power provided by a PV power generation system depends on the solar radiation and temperature. In tropical countries like India, availability of solar power is in abundance and a PV system can meet the emerging power demand. However, there is an initial expense involved in the installation and erection of solar PV system, even though, they can operate with nearly nil running and maintenance cost. The PV panel itself contributes to about 57% of the total cost of the system, the cost of battery and inverter (with Maximum Power Point Tracking (MPPT) control) around 30% and 7%, respectively [1-3]. Continuous research is going in the area of PV innovation keeping in mind the end goal to reduce cost endeavours. It is anticipated that the PV per watt cost will diminish radically by the year 2020 as per IEEE spectrum report. To reduce the total initial investment cost of the PV system, it is mandatory to reduce the cost [4-5] of other associated components (DC-DC converter, inverter module, battery backup and instrumentation).The primary goal of this paper is to produce quality electricity from solar PV to reduce dependence on fossil fuels and to reduce the cost of energy consumption by connecting the PV system to grid. Elimination of usage of storage batteries in on-grid solar PV system and complicated MPPT control reduces the total cost investment per watt.

The investment cost of the on-grid system can also be reduced by decreasing the number of power conversion stages [6] and the components count involved with every stage. As transformers provide an inherent protection against DC injected into the grid, the inverters without transformer require extra hardware in order to limit the DC injection to the lowest permitted limit (also different from country to country due to their regulations).In any case, the transformer-less design is electrically more efficient, as the transformer involves reduction of approximately 2% of peak proficiency. In this proposed grid-tied (on-grid) inverter, the circuit is outlined without a transformer. In addition, the transformerless PV grid-connected inverter topology can support a wide range of input voltages, high efficiency, lower cost, smaller size, less weight and high reliability when compared with transformer based configuration [7-9]. In audit papers [10-12], a verifiable outline of some past, present and future power inverter topologies for interfacing PV modules to the grid were discussed. In review paper [13-14], the authors focused on small string and module integrated types of inverter topologies and their efficiency. In boost half bridge micro-inverter [15-16], for grid-connected PV systems, has minimal usage of semiconductor devices, circuit simplicity, and simple control. The boost half bridge PV based inverter has capable features of low cost and high reliability. Moreover, the current injected into the grid is controlled precisely and also, stiff in harmonics free.

From the power source perspective, the traditional inverters are voltage-source converters (truncated as V-source converters) and current-source converters (truncated as I-source converters). The V-source converters and I-source converters are generally utilized yet, have some theoretical and practical hindrances and confinement [17-19]. Additionally, the shoot-through issue is involved in a conventional bridge type voltage source inverter. In order to overcome the above mentioned problem, a Z-source inverter [20-22] has been proposed. In any case, the Z-source inverter needs two input inductors and two input capacitors to boost the input voltage. In addition, the in-rush current and resonance between the Z-capacitors and Z-inductors at start up may wreck the power components, and since, the input capacitor voltage needs to be controlled, overall control is more complicated with regular inverters. Finally, for converter configuration [23-25], the authors clearly provides group of various high competence solitary stage DC to AC inverters, and have also discussed the reduction of switching losses in high frequency switching converters. However, the number of passive components still cannot be reduced.

Normally, the current generated by a grid interactive PV-inverter contains harmonics which lead to power quality problem. For the harmonic issue [26-27], the authors present a single phase distortion reduction schemes by implementing generation side power quality conditioner in order to meet the IEEE and IEC norms.

Keeping in mind the end goal to beat the previously mentioned obstructions of grid-connected inverter topologies, a novel inverter topology is proposed in this work. This topology is developed from the scheme exhibited in [28-29]. The advantages of the proposed work are as follows:

i. Extraction of power from two distinctive PV panels.
ii. The inverter working in buck mode and buck-boost mode can support a wide range of voltage variations.
iii. Need only just four switches, and hence, less switching losses.
iv. No need of bulky transformer, and hence, the weight of the inverter is less.
v. Reverse power flow can be controlled by this proposed configuration, and hence, no need of diodes.
vi. The overall cost of the inverter is less because of fewer components.

## 2. Operating Principle of the Proposed Inverter

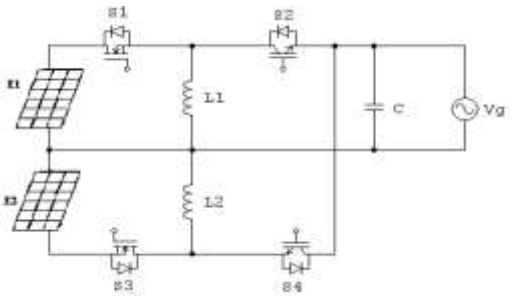


**Fig. 1.** Proposed DC/AC grid tied inverter.

The proposed single stage "DC/AC grid tied inverter" is presented to demonstrate the elementary concept of the inverter briefly as shown in Fig. 1. Operating modes of the converter can be explained in two modes, that is, buck mode and buck-boost mode. For simplification, voltages from $PV_1$ and $PV_2$ are considered as $E_1$ and $E_2$ respectively throughout this paper. The circuit configuration is similar to neutral point clamped structure. This structure avoids leakage current flow due to parasitic capacitances existing between ground terminal and the PV panels.

*2.1 Buck mode-Negative half and Positive half cycle operation of the grid voltage*

During sunshine condition, the insolation value will be more. Proportionately the PV panel voltage induced also is more. If the voltage input given to the converter is higher than the AC grid voltage $V_g$ (i.e $|E_1|$ or $|E_2| \geq V_g$,) then, the converter works in the buck mode. Fig. 2(a) shows the equivalent circuit corresponding to the generation of negative half cycle of the grid voltage $V_g$. In this mode, the switches $S_1$ and $S_2$ are operated in buck mode and the switches $S_3$ and $S_4$ will stay in 'OFF' condition. Here, the $S_1$ works at higher frequency to get sinusoidal negative half cycle of grid current and voltage waveform, and for negative half cycle, $E_1$ alone provides total energy to the grid. Correspondingly, Fig. 2(b) shows next half of the equivalent circuit which is responsible for delivering the positive half cycle of the grid voltage $V_g$. In this mode, the switches $S_3$ and $S_4$ work in buck mode and the switches $S_1$ and $S_2$ will stay in 'OFF' condition. Here the $S_3$ works at a higher frequency to achieve the sinusoidal positive half cycle of grid current and voltage waveform while, $E_2$ alone gives total energy to the grid. In this pure buck mode, the converter switches $S_1$ and $S_3$ work at the duty cycle lower than 50 %.

*2.2 Buck-Boost mode operation-Negative half and Positive half cycle operation of the grid voltage*

During cloudy condition, the insolation value will be less. Proportionately the PV panel voltage induced also less. If the voltage input given to the converter is lower than the AC grid voltage $V_g$ (i.e $|E_1|$ or $|E_2| < V_g$,) then, the converter will work in the buck and boost mode together, then the converter control becomes a slightly more complex, here the working process can be divided in to six parts for one cycle is explained as shown in Fig. 3.

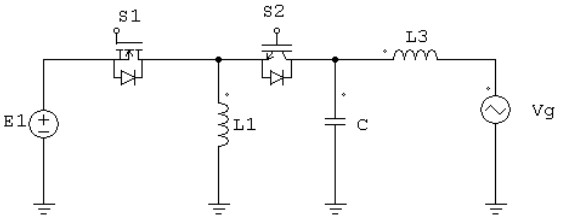


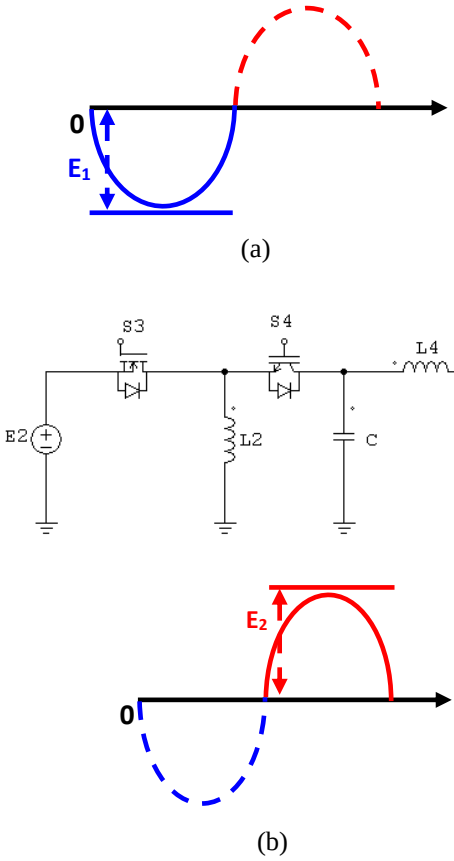


**Fig. 2.** Equivalent circuits and output waveforms when $E_1$ and $E_2$ are greater than grid voltage. a. During negative half cycle. b. Duration positive half cycle.

*2.3 Negative half cycle operation of the grid voltage*

When the instantaneous value of the grid voltage is lower than the input DC voltage (during $T_1$ & $T_3$) the converter operates in buck mode and likewise if the grid voltage is higher than the input DC voltage (during $T_2$) the converter operates in boost mode. In this both modes of time intervals the switches $S_1$ and $S_2$ stayed in turn 'ON' condition; other switches are in 'OFF' condition. Here the $S_1$ is working at higher frequency to achieve the sinusoidal negative half cycle. To get negative half cycle $E_1$ alone provides total energy to the grid. In this mode, the converter switch $S_1$ works at the duty cycle lower than that of 50 %.In this period the energy stored in the boost inductor $L_1$ is utilized and controlled absolutely through $S_2$ switch. In this mode also $S_1$ remains in 'ON' position but the frequency of switching alone differs. $S_2$ works as a diode to prevent reverse flow of power from grid and will be operating at the duty cycle greater than 50 % to a maximum of 99 %.

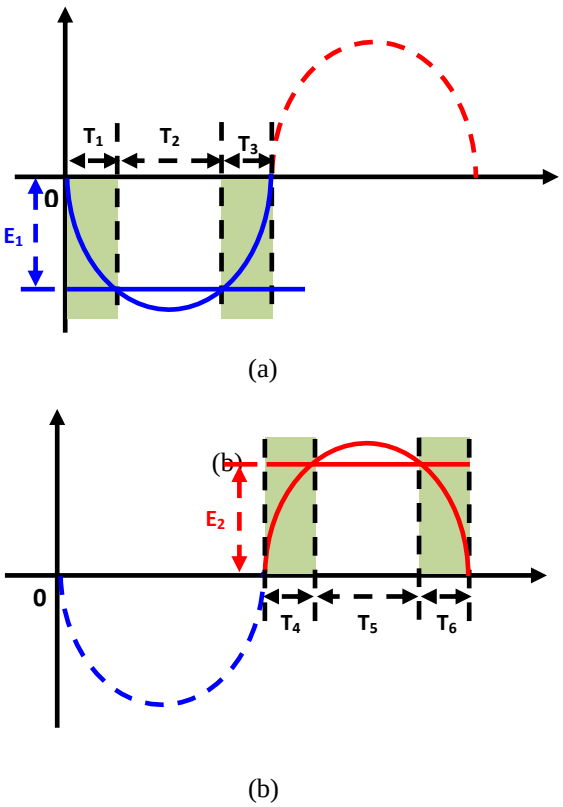


**Fig. 3.** Working sequences when $E_1$ and $E_2$ are lower than the grid voltage. a. Time durations of negative cycle. b. Time durations of positive cycle.

*2.4 Positive half cycle operation of the grid voltage*

Correspondingly, when the instantaneous value of the grid voltage is lower than the input DC voltage (during $T_4$ & $T_6$) the converter operates in buck mode and likewise if the grid voltage is higher than the input DC voltage (during $T_5$) the converter operates in boost mode. In both these modes of time intervals the switches $S_3$ and $S_4$ stayed in turn 'ON' condition; other switches are in 'OFF' condition. Here, the switch $S_3$ is works at higher frequency to achieve the sinusoidal negative half cycle. To get negative half cycle $E_2$ alone provides total energy to the grid. In this mode, the converter switch $S_3$ will work at the duty cycle lower than that of 50 %.In this period the energy stored in the boost inductor $L_2$ is utilized and controlled absolutely through $S_4$ switch. In this mode also $S_3$ remains in 'ON' position but the frequency of switching only differs. $S_4$ works as diode to prevent reverse flow of power from grid and will be operating at the duty cycle greater than 50 % to a maximum of 99 %.

## 2. Control Strategy

*3.1 Converter modelling.*

During the time intervals of $T_1$, $T_3$, $T_4$ and $T_6$ as shown in Fig. 3, the converter completely acts as a voltage source inverter connected to the grid through with LC-filter. The control part is analysed considering current source inverter as controllable input during the time intervals of $T_2$ and $T_5$. Here, small signal model is assumed for analysis, where small signal modelling works only for the constant signal output. Here, the grid is assumed to be in the steady state. The only changing factor in the grid is frequency, but the grid frequency is too small when compared to the switching high frequency of the inverter.

It is noticed during $T_2$ and $T_5$, the equivalent circuits are similar. As shown in Fig. 4 and Fig. 5, the general common equivalent circuit is followed for modelling, where $E_1$ and $E_2$ represents the DC voltages of solar PV, $i_1$ denotes the DC current through the inductor $L_1$, and while, simplifying the analysis process the semiconductors impacts are omitted.

Applying KVL

$$L_1 \frac{di_1(t)}{dt} = -R_1 i_1(t) + E_1(t) \tag{1}$$

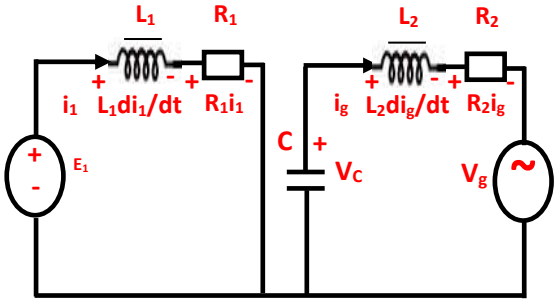


**Fig. 4.** Equivalent circuit during $S_1$ is 'ON' at time interval of ([t, t+DTs]).

$$C \frac{dVc(t)}{dt} = -i_g(t) \tag{2}$$

$$L_2 \frac{di_g(t)}{dt} = V_c(t) - R_2 i_g(t) - V_g(t) \tag{3}$$

From (1), (2) & (3) the state equation can be described as,

$$\begin{pmatrix} L_1 & 0 & 0 \\ 0 & C & 0 \\ 0 & 0 & L_2 \end{pmatrix} \frac{d}{d_t} \begin{pmatrix} i_{1(t)} \\ V_{c(t)} \\ i_{g(t)} \end{pmatrix} = \begin{pmatrix} -R_1 & 0 & 0 \\ 0 & 0 & -1 \\ 0 & +1 & -R_2 \end{pmatrix} \begin{pmatrix} i_{1(t)} \\ V_{c(t)} \\ i_{g(t)} \end{pmatrix} + \begin{pmatrix} 1 & 0 & 0 \\ 0 & 0 & 0 \\ 0 & 0 & -1 \end{pmatrix} \begin{pmatrix} E_{1(t)} \\ 0 \\ V_{g(t)} \end{pmatrix} \tag{4}$$

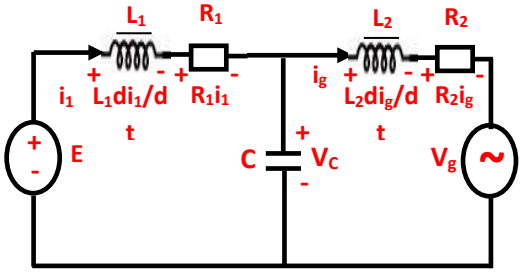


**Fig. 5.** Equivalent circuit during $S_1$ is 'OFF' at time interval of [t+DTs, t+Ts].

Applying KVL

$$L_1 \frac{di_1(t)}{dt} = -R_1 i_1(t) - Vc(t) + E_1(t) \quad (5)$$

$$C \frac{dVc(t)}{dt} = i_1(t) - i_g(t) \quad (6)$$

$$L_2 \frac{di_g(t)}{dt} = V_c(t) - R_2 i_g(t) - V_g(t) \quad (7)$$

From (5), (6) & (7) the state equation represented as,

$$\begin{pmatrix} L_1 & 0 & 0 \\ 0 & C & 0 \\ 0 & 0 & L_2 \end{pmatrix} \frac{d}{d_t} \begin{pmatrix} i_{1(t)} \\ V_{c(t)} \\ i_{g(t)} \end{pmatrix} = \begin{pmatrix} -R_1 & -1 & 0 \\ 1 & 0 & -1 \\ 0 & 1 & -R_2 \end{pmatrix} \begin{pmatrix} i_{1(t)} \\ V_{c(t)} \\ i_{g(t)} \end{pmatrix} + \begin{pmatrix} 1 & 0 & 0 \\ 0 & 0 & 0 \\ 0 & 0 & -1 \end{pmatrix} \begin{pmatrix} E_{1(t)} \\ 0 \\ V_{g(t)} \end{pmatrix} \quad (8)$$

where $R_1$ and $R_2$ are the equivalent resistors of $L_1$ and $L_2$ respectively, current through $L_1$ and grid current are $i_1(t)$ and $i_g(t)$ respectively, and the capacitor voltage is $V_c(t)$.

*3.2 Control diagram of proposed grid tied inverter*

In this paper, to keep up the AC voltage constant for line and load variations, a PI controller along with the hysteresis current controller has been designed and implemented for solar PV fed grid system. To get the desired output, the values of $K_p$ and $K_i$ must be picked by apriori test. In the closed loop using a PI controller, the overshoot and settling time are less compared to the open loop, and also, less oscillatory.

The hysteretic current control shown in Fig. 6 is considered here due to the least complex and quickest control method. This control approach has fast response and robust with simple design and easy implementation. Owing to the above mentioned reason this control method requires only fewer components and lesser theoretical analysis for implementation, and also, reduces the design effort.

Fig. 7 shows the control scheme for the proposed converter. The solar PV input DC voltages $E_1$, $E_2$ and the grid voltage $V_g(t)$ are alone considered. If the PV voltage is greater than the voltage magnitude of grid, then the "Buck" mode reference current can be calculated as

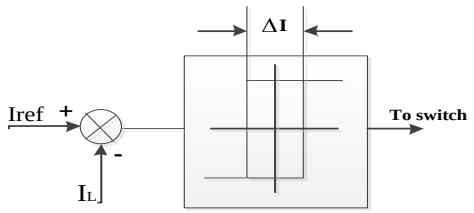


**Fig. 6.** Hysteresis current control

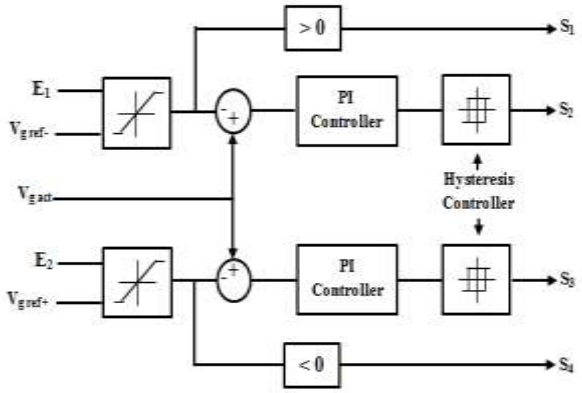


**Fig. 7.** Control diagram for the proposed converter.

$$i_{Ref\ \text{Buck}} = \frac{\left|V_g(t)\right|^2}{R_f} \quad (9)$$

Similarly, when the solar PV input DC voltage is lesser than the voltage magnitude of grid $V_g$, the "Boost" mode current reference current can be calculated as

$$i_{Ref\ \text{Boost}} = \frac{\left|V_g(t)\right|^2}{R_f \square E_1 (or E_2)} \quad (10)$$

The grid voltage is sensed and divided into two, ($V_g$<0) and ($V_g$>0). Now,

$$\left.\begin{aligned} V_{grid} &= (V_g > 0) \\ V_{grid} &= (V_g < 0) \end{aligned}\right\} \quad (11)$$

The upper half bridge grid voltage $V_g$ is composed of the output signal and the error is manipulated with a PI controller. The reference current is applied to a hysteresis band to generate the gate signal to the switches. Here the $S_1$ and $S_3$ are operated for buck-boost mode with a high switching frequency. The switches $S_2$ and $S_4$ are operated to avoid reverse flow of power from grid and are operated with low switching frequency.

## 4. Simulation Results

To evaluate the performance of the proposed grid-tied inverter, a detailed simulation study has been carried out in MATLAB/Simulink platform. Various components and parameters were considered for the simulation studies and provided in Table. 1. Fig. 8 shows the MATLAB/Simulink model.

When the instantaneous voltage of AC grid is lesser than solar PV input DC voltage (buck mode operation), the steady-state utility grid voltage $V_g(t)$ and DC input voltages ($E_1$=$E_2$=350V) waveforms are depicted in Fig. 9 with the constant frequency of 50 Hz.

**Table.1** Simulation Results

| Description | Parameter | Typical | Units |
|---|---|---|---|
| DC input Voltage | $V_{in}$ | 180-350 | V |
| Grid Voltage | $V_{grid}$ | 230 | V |
| Inductor | $L_1 = L_2$ | 0.1 | mH |
| Capacitor | $C_1 = C_2$ | 56 | µF |
| Switching Frequency | f | 20 | kHz |
| Grid Frequency | $f_g$ | 50 | Hz |
| Efficiency | η | >97 | % |

Similarly, when the instantaneous voltage of AC grid is greater than solar PV input DC voltage (buck-boost mode), $E_1$=$E_2$=190V, the steady state simulated results are illustrated in Fig. 10 and grid voltage $V_g(t)$ with constant frequency of 50 Hz. Both light load and dense load conditions are tested to check the performance of the controller stability.

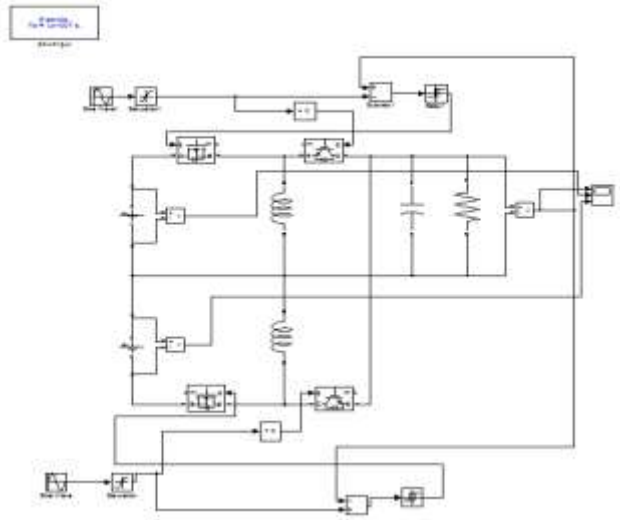

**Fig. 8.** MATLAB/Simulink model diagram

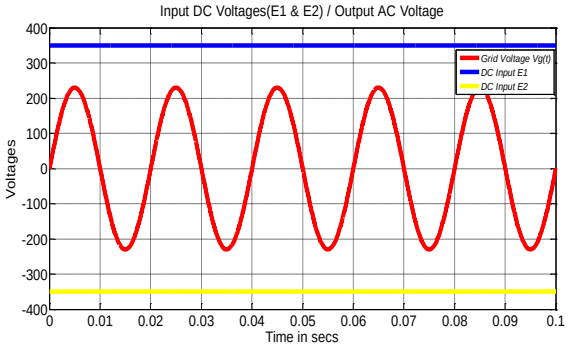


**Fig. 9.** Simulated maximum input DC voltage ($E_1$ and $E_2$) and grid voltage $V_g(t)$ when $E_1$=$E_2$=350V.

The energy stored in the boost inductors of $L_1$ & $L_2$ are controlled absolutely through $S_2$ & $S_4$ switches and the waveforms are shown in Fig. 11 and Fig. 12 respectively. The DC inductor currents $iL_1$ and $iL_2$ are also shown in that figures.

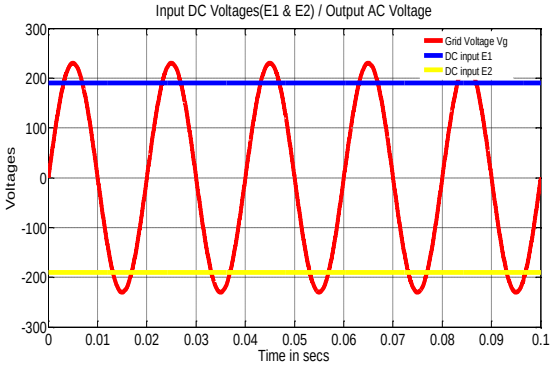


**Fig. 10.** Simulated output when input DC voltage ($E_1$ and $E_2$) and grid voltage $V_g(t)$ when $E_1$=$E_2$=190V.

Fig. 13 shows the measured input AC utility grid voltage $i_g(t)$, at full load with constant frequency of 50 Hz, demonstrates a tendency of good current waveform.

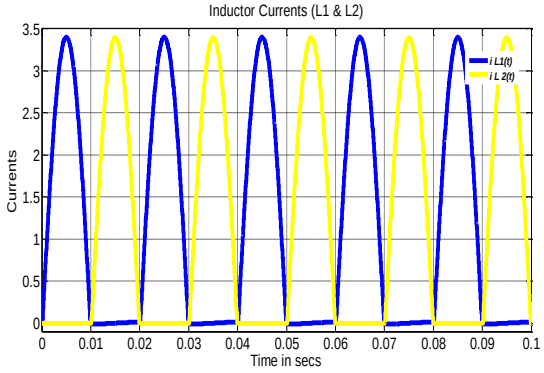


**Fig. 11.** DC currents of inductors $iL_1$ and $iL_2$, when $E_1$=$E_2$=350V.

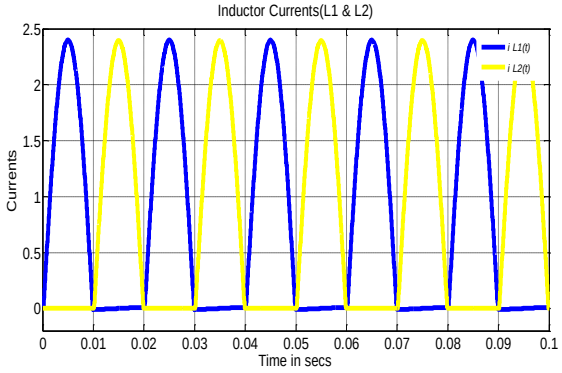


**Fig. 12.** DC currents of inductors $iL_1$ and $iL_2$, when $E_1$=$E_2$=190V.

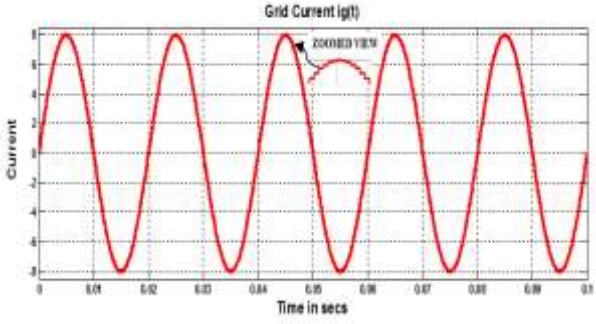


**Fig. 13**. Utility Grid injected current $i_g(t)$ at full load.

The illustration in Fig. 14 shows the Fast Fourier Transform (FFT) analysis of the grid current $i_g(t)$ at steady state condition. The histogram shows the amplitude of the fundamental and harmonic components. The distortion value of the current is presented as Total Harmonic Distortion (THD). By analysing, one can note that the integrated current is sinusoidal with low THD with the presence of fewer odd harmonics, and also, the current THD of the system meets IEC guidelines limits indicated by the standard IEC 61000-3-2 (7% for currents up to 16A). Thus, the system improves harmonic distortion factor by reducing the lower order harmonics. The grid voltage $V_g(t)$ and the inverter output power is then synchronized to the grid through Zero Crossing Detector (ZCD).

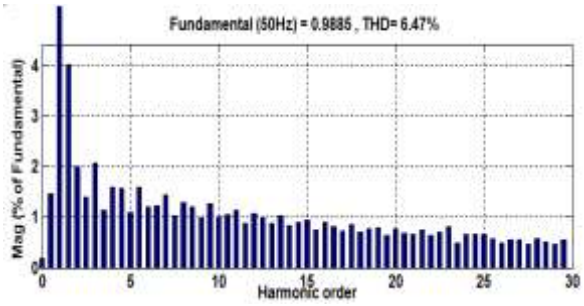


**Fig. 14**. FFT analysis of grid current THD.

## 5. Experimental Results

The anticipated working principles and theoretical analysis of the proposed novel topology has been realized with a prototype of 2kW capacity converter along with two set PV panels capacity of 2kW (8×250 watts) each taken for experimental study from the research laboratory.

**Table.2** Prototype Parameters

| Description | Parameter | Typical | Units |
|---|---|---|---|
| PV Panel Voltage | $V_{in}$ | 50-90 | V |
| Grid Voltage | $V_{grid}$ | 230 | V |
| Grid Frequency | f | 49.6-50 | Hz |
| Power Factor | PF | >0.95 | - |
| Current THD at Full Load (8.08A) | $I_{THD}$ | <7 | % |
| Input PV Power | $M_{PV.P}$ | 2 | kW |
| Output Power | $P_{out}$ | 1.93 | kW |
| Switching Frequency ($S_1$ & $S_3$) | f | 20 | kHz |
| Efficiency at Full load (8.08A) | η | 96.5 | % |

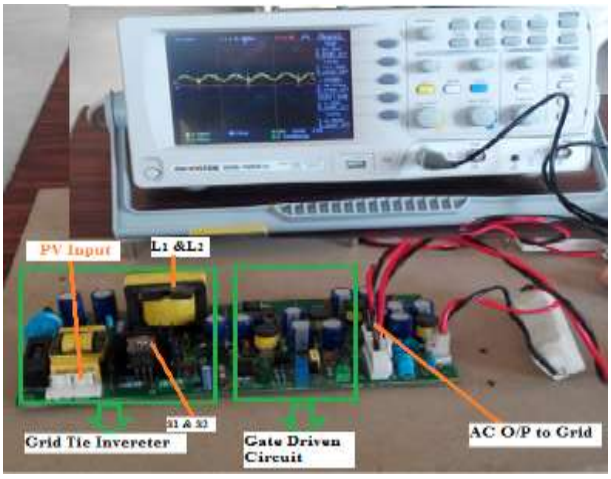


**Fig.15**.The hardware setup of the proposed Grid Connected Inverter System.

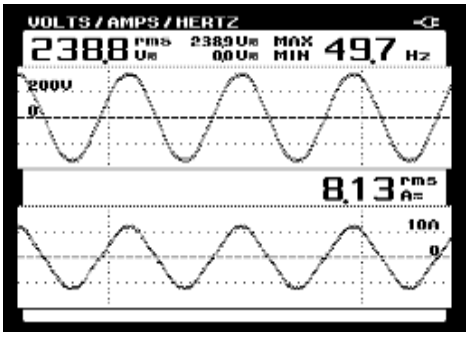


**Fig. 16**. Photograph of grid voltage and load current waveform.

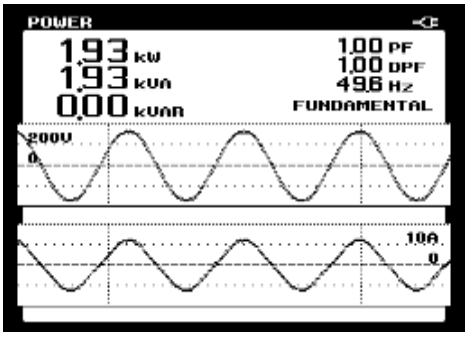


**Fig. 17.** Photograph of output real power, apparent power and power factor.

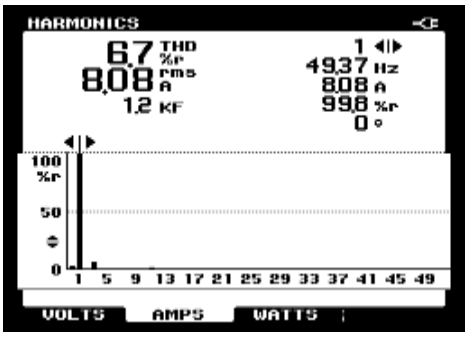


**Fig. 18.** The THD factor of load current waveform of the proposed system.

The experimental results have been taken on the prototype with parameters listed in Table.2 based on available research centre facilities. The hardware setup of the proposed work is depicted in Fig. 15.The quality of the power extracted from the proposed converter is measured utilizing the power quality analyser. Here the input power is taken from two PV panels. The prototype kit is tested on maximum insolation value of 880 W/m$^2$.The output of the system seems to be 1.93kW at a full load of unity power factor load. The Fig. 16 outlines the waveforms for the grid voltage and inverter injection current respectively. Fig. 17 depicts the real power, apparent power, reactive power and power factor and efficiency of the system at the most of 96.5 %.The inverter voltage is intended to work with 50Hz grid frequency. While observing the grid parameters, the current waveform is sinusoidal, and furthermore, in phase with the grid voltage. It is evident from the Fig. 18, the THD value measured using the power quality analyser complies with the IEC guidelines.

## 6. Conclusions

The cost-effective novel grid-tied transformerless inverter, which has the ability to harvest maximum power from two distinctive PV panels working under equal and in addition unequal climatological circumstances, is exhibited. The proposed inverters would upkeep extensive deviation in panel voltages. Grasped power from two PV panels is conditioned using PI along with hysteresis controller is fed in to the grid all together after confirming the grid synchronisation conditions. It is realized from the experimental outcomes that the THD value of the output current is as per the IEC norms. Thus, it can be said that the transferred power to the grid is in good quality. Subsequently, size of the passive filter is considerably reduced due to the harmonic factor. The simulated performance of the converter is confirmed using experimental output proof on a research facility model. Ultimately, the co-ordinated activity and a blend of technologies reduced the components count, and this new converter topology is designed on the premise of cost-efficiency.

## References

[1] J. H. R. Enslin, M. S. Wolf, D. B. Snyman and W. Swiegers, "Integrated photovoltaic maximum power point tracking converter," IEEE Transactions on Industrial Electronics, vol. 44, no. 6, pp. 769-773, Dec 1997.

[2] Chub, D. Vinnikov, R. Kosenko and E. Liivik, "Wide input voltage range photovoltaic microconverter with reconfigurable buck–boost switching stage," IEEE Transactions on Industrial Electronics, vol. 64, no. 7, pp. 5974-5983, July 2017.

[3] Y. Furukawa, T. Shirakawa, F. Kurokawa and I. COLAK, "A new quick response digital control dc-dc Converter with dynamic unstable gain", IEEE 4th International Conference on Renewable Energy Research and Application (ICRERA'15), 22-25 November 2015.

[4] S.Kirmani, M.Jamil and I.Akhtar, "Effective low cost Grid-Connected Solar Photovoltaic System to Electrify the Small Scale industry/Commercial Building," International Journal of Renewable Energy Research, vol.7, no.2, March 2017.

[5] P. Satapathy, S. Dhar and P. K. Dash, "An evolutionary online sequential extreme learning machine for maximum power point tracking and control in multi-PV microgrid system," Renewable Energy Focus, vol. 21, pp. 33-53, October 2017.

[6] Y. Furukawa, H. Nakamura, H. Eto, I. Colak and F. Kurokawa, "Step response of high feedback gain changeable control DC-DC converter," IEEE 6th International Conference on Renewable Energy Research and Application (ICRERA'17), 597-601, November 2017.

[7] Dube, M. Rizwan and M. Jamil, "Analysis of single phase grid connected PV system to identify efficient system configuration," 2016 Second International Innovative Applications of Computational Intelligence on Power, Energy and Controls with their Impact on Humanity (CIPECH), Ghaziabad, 2016, pp. 173-177.

[8] Z. Ozkan and A.M. Hava, "Classification of grid connected transformerless PV inverters with a focus on the leakage current characteristics and extension of topology families," Journal of Power Electronics, vol. 15, no.1, pp. 256-267, January 2015.

[9] S. Deng, Y. Sun, J. Yang, Q. Zhu and M. Su, "Optimized hybrid modulation strategy for ac bypass transformerless single-phase PV inverters," Journal of Power Electronics, vol. 16, no. 6, pp. 2129-2138, November 2016.

[10] Linss T. Alex, V. Jaikrishna, Subranhsu Sekhar Dash and R. Sridhar, "Design and analysis of Push-pull-Flyback interleaved converters for photovoltaic system," IEEE 6th International Conference on Renewable Energy Research and Application (ICRERA'17), 757-761, November 2017.

[11] Z. Ahmad and S. N. Singh, "Comparative analysis of single phase transformerless inverter topologies for grid connected PV system," Solar Energy, vol. 149, pp. 245-271, June 2017.

[12] J. F. Ardashir, M. Sabahi, S. H. Hosseini, F. Blaabjerg, E. Babaei and G. B. Gharehpetian, "A single-phase transformerless inverter with charge pump circuit concept for grid-tied PV applications," IEEE Transactions on Industrial Electronics, vol. 64, no. 7, pp. 5403-5415, July 2017.

[13] M. Islam, S. Mekhilef and M. Hasan, "Single phase transformerless inverter topologies for grid-tied PV system: A review," Renewable and Sustainable Energy Reviews, vol. 45, pp. 69-86, May 2015.

[14] O. Noureldeen and A.M.A. Ibrahim, "Performance Analysis of Grid Connected PV/Wind Hybrid Power System during Variations of Environmental Conditions

and Load," International Journal of Renewable Energy Research, vol.8, no.1, March 2018.

[15] S. Mishra, D. Pullaguram, S. A. Buragappu and D. Ramasubramanian, "Single-phase synchronverter for a grid-connected roof top photovoltaic system," IET Renewable Power Generation, vol. 10, no. 8, pp. 1187-1194, September 2016.

[16] Z. Ahmad, and S. N. Singh, "An improved single phase transformerless inverter topology for grid connected PV system with reduce leakage current and reactive power capability," Solar Energy, vol. 157, pp. 133-146, November 2017.

[17] J. Jana, H. Saha and K. D. Bhattacharya, "A review of inverter topologies for single-phase grid-connected PV systems," Renewable and Sustainable Energy Reviews, vol. 72, pp. 1256-1270, May 2017.

[18] J. M. A. Myrzik and M. Calais, "String and module integrated inverters for single-phase grid connected photovoltaic systems - A review," IEEE Bologna Power Tech Conference Proceedings, vol. 2, pp. 1-8, 2003.

[19] S. Jiang, C. Dong, Y. Li and F. Peng, "Grid-connected boost-half-bridge photovoltaic microinverter system using repetitive current control and maximum power point tracking," IEEE Transactions on Power Electronics, vol. 27, no. 11, pp. 4711–4722, November 2012.

[20] Florescu, O. Stocklosa, M. Teodorescu, C. Radoi, D. A. Stoichescu and S. Rosu, "The advantages, limitations and disadvantages of Z source inverter," in IEEE CAS 2010 Proceedings (International Semiconductor Conference),Sinaia, pp. 483-486, 2010.

[21] P.Nammalvar and S.Ramkumar, "Performance and analysis of Z-source inverter based grid connected solar power system," International Journal of Applied Engineering Research, vol.10, no.12, pp. 32259-32274, July 2015.

[22] AV. Ho and TW. Chun, "Modified capacitor-assisted z-source inverter topology with enhanced boost ability," Journal of power Electronics, vol. 17, no. 5, pp.1195-1202, September 2017.

[23] W. Wu, J. Ji and F. Blaabjerg, "Aalborg Inverter - A new type of "buck in buck, boost in boost" grid-tiedinverter," IEEE Transactions on Power Electronics, vol. 30, no. 9, pp. 4784-4793, March 2015.

[24] MI . Hamid and A. Jusoh, "Reduction of waveform distortion in grid-injection current from single-phase utility interactive PV-inverter," Energy Conversion and Management, vol. 85, pp. 212-226, September 2014.

[25] M. Khatri and A. Kumar, "Experimental Investigation of Harmonics in a Grid-Tied Solar Photovoltaic System," International Journal of Renewable Energy Research, vol.7, no.2, March 2017.

[26] P. Nammalvar and S. Ramkumar, "Parameter Improved Particle Swarm Optimization Based Direct-Current Vector Control Strategy for Solar PV System," Advances in Electrical and Computer Engineering, vol.18, no.1, pp.105-112, February 2018.

[27] S. Moulahoum, O. Aissa, I. COLAK, B. Babes and N. Kabache, "Analysis, design and real-time implementation of shunt active power filter for power quality improvement based on predictive direct power control", 5th International Conference on Renewable Energy Research and Application (ICRERA'16), 20-23 November 2016.

[28] G.M. Vargas-Gil, C. Juan C. Colque, A. J. Sguarezi and R. M. Monaro, "Sliding mode plus PI control applied in PV systems control," IEEE 6th International Conference on Renewable Energy Research and Application (ICRERA'17), 562-567, November 2017.

[29] D. Debnath and K. Chatterjee "Maximising power yield in a transformerless single-phase grid connected inverter servicing two separate photovoltaic panels," IET Renewable Power Generation, vol. 10, no. 8, pp. 1087-1095, September 2016.